Available online at www.sciencedirect.com
ScienceDirect
Pattern Recognition Letters 27 (2006) 1732–1743
Pattern Recognition Letters
www.elsevier.com/locate/patrec

On minimum variance thresholding

Z. Hou [a,*], Q. Hu [b], W.L. Nowinski [b]

[a] Department of Interactive Media, Institute for Infocomm Research, 21 Heng Mui Keng Terrace, Singapore 119613, Singapore
[b] Biomedical Imaging Lab, Singapore Bioimaging Consortium, 11 Biopolis Way, #02-02 Helios, Singapore 138667, Singapore

Received 24 November 2004; received in revised form 24 March 2006
Available online 21 June 2006

Communicated by Y.J. Zhang

Abstract

Variance-based thresholding methods could be biased from the threshold found by expert and the underlying mechanism responsible for this bias is explored in this paper. An analysis on the minimum class variance thresholding (MCVT) and the Otsu method, which minimizes the within-class variance, is carried out. It turns out that the bias for the Otsu method is due to differences in class variances or class probabilities and the resulting threshold is biased towards the component with larger class variance or larger class probability. The MCVT method is found to be similar to the minimum error thresholding.

Keywords: Image thresholding; Centroid; Class variance; Class probability

1. Introduction

Thresholding is a technique frequently applied to image segmentation. The implicit assumption is that the intensity is similar within an object and different between different objects. Thus, in the gray-level histogram each object could appear as a bell-shape mode and the threshold can be selected as the valley between modes. The valley can be detected directly (Prewitt and Mendelsohn, 1966; Weszka and Rosenfeld, 1979; Rosenfeld and Torre, 1983; Wu and Manmatha, 1998). More often, it is formulated as an optimization problem and the valley is identified indirectly. The minimum error thresholding (Chow and Kaneko, 1972; Nakagawa and Rosenfeld, 1979; Kittler and Illingworth, 1986; Cho et al., 1989; Ye and Danielsson, 1988) assumes the intensity distribution of an object as the Gaussian and searches the threshold by minimizing the Bayes error. The main problem of this method is that the assumed Gaussian model could be violated in practice due to various perturbations and results in the so-called model bias. There are also attempts using the maximum entropy principle (Pun, 1981; Wong and Sahoo, 1989; Shanbhag, 1994), the moment-preserving principle (Tsai, 1985) and the fuzzy logic (Huang and Wang, 1995; Cheng and Chen, 1999; Saha and Udupa, 2001; Tobias and Seara, 2002; Wang et al., 2002). In addition, the above methods could be integrated, resulting in more complicated methods. Cheng and Chen (1999) investigated the hybrid of fuzzy logic and the maximum entropy principle. And the hybrid of Bayesian formulation and the maximum entropy principle has been reported by Chang et al. (2002).

A popular method is the Otsu method (Otsu, 1979), which minimizes the within-class variances for threshold selection. Yan (1996) pointed out that the Otsu method (Otsu, 1979), the cross entropy method (Li and Lee, 1996) and the Huang and Wang method (Huang and Wang, 1995) could be formulated in a unified framework. Although a number of thresholding techniques have been proposed in the past decades, the Otsu method is still among the most popular for its simplicity and efficiency. Nonetheless, experiments often show that the Otsu method could be biased for reasons yet to be explored.

* Corresponding author. Tel.: +65 6874 8549; fax: +65 6774 4990.
E-mail address: zhou@i2r.a-star.edu.sg (Z. Hou).

0167-8655/$ - see front matter © 2006 Elsevier B.V. All rights reserved.
doi:10.1016/j.patrec.2006.04.012

As an attempt to understand the mechanism responsible for the thresholding bias of the Otsu method, we analyze two minimum variance thresholding methods: minimum within-class variance (i.e., the Otsu method) and minimum class variance in this paper. The former is equivalent to maximizing the between-class variance, since the total variance (the sum of the within-class variance and the between-class variance) is constant for different partitions. Here, the terms of within-class variance and between-class variance are adopted from a popular statistical branch, analysis of variance (commonly known as ANOVA), which is widely used for data mining in a variety of science and engineering applications, including image processing (Kurz and Benteftifa, 1997). In ANOVA, the two terms are usually named as the within-group variance and the between-group variance. As for the second method, the minimum class variance thresholding (MCVT), it can be regarded as a generalized Otsu method, where the term of class variance follows the precise definition of variance for a class. Analysis on both methods reveals that the bias in the Otsu and the MCVT methods is affected by the class probability and the class variance. In particular, the Otsu method is biased towards the component with larger class probability or larger class variance. Such factors have less impact on the MCVT method, thereby, the latter could result in more accurate results for images with homogeneous noise and multi-modal histogram. The difference between the two methods is due to the different mechanisms in the process of thresholding. The minimum class variance thresholding method considers the average distance relative to the class variance for threshold determination, whereas the Otsu method takes account of the absolute distance. The analysis has been verified through experiments on synthetic and real images.

The paper is organized as follows. In Section 2, we first formulate the variance-based thresholding methods, including the minimum within-class variance thresholding (namely the Otsu method) and the MCVT method for bi-level thresholding. Then, an analysis of these two methods is given, where the features of both methods and the advantages of the MCVT method over the Otsu method are deduced. After that, the MCVT method is generalized to multi-level thresholding. Section 3 describes the performance investigation over synthetic and real images. Finally, the paper is concluded in Section 4.

2. Method

Let I denote a gray-scale image with gray levels $\Omega = \{r_i, i = 0, \ldots, L-1 | r_0 < r_1 < \cdots < r_{L-1}\}$, and the histogram be $\{h_i\}$. For convenience, we first consider a bi-level thresholding problem. Suppose $r_0 < r_k < r_{L-1}$. A two-level partition of the gray levels is defined as follows. Let $C_1 = \{r_0, \ldots, r_k\}$ and $C_2 = \{r_{k+1}, \ldots, r_{L-1}\}$. Then C_1 and C_2 is a two-level partition of Ω. Clearly, $C_1 \subset \Omega, C_2 \subset \Omega$ and $C_1 \cup C_2 = \Omega$, $C_1 \cap C_2 = \emptyset$.

For each component, the class probability

$$P_i = \begin{cases} \sum_{j=0}^{k} h_j & i = 1, \\ \sum_{j=k+1}^{L-1} h_j & i = 2, \end{cases} \tag{1}$$

the class mean

$$\mu_i = \begin{cases} \sum_{j=0}^{k} r_j h_j \Big/ P_1 & i = 1, \\ \sum_{j=k+1}^{L-1} r_j h_j \Big/ P_2 & i = 2, \end{cases} \tag{2}$$

and the class variance

$$D_i = \begin{cases} \sum_{j=0}^{k} (r_j - \mu_1)^2 h_j \Big/ P_1 & i = 1, \\ \sum_{j=k+1}^{L-1} (r_j - \mu_2)^2 h_j \Big/ P_2 & i = 2. \end{cases} \tag{3}$$

The Otsu method selects the threshold by minimizing

$$\min_{r_k} (P_1 D_1 + P_2 D_2). \tag{4}$$

In (4), $\sum P_i D_i$ is called the within-class variance, in a fashion similar to the definition in ANOVA. It should be pointed out that within-class variance is not the class variance. Naturally, we can construct the thresholding method which minimizes the class variances:

$$\min_{r_k} (D_1 + D_2). \tag{5}$$

However, the criterion (5) is generally ignored. The reason why the criterion (4) is preferred may be the theorem regarding the decomposition of variances in ANOVA, which states that the total variance is the sum of the within-class variances and the between-class variances, and remains constant in the process of optimization (see statistical textbooks or Otsu (1979) for a reference). Thus, minimizing the within-class variances is equivalent to maximizing the between-class variances. For the variance used in the criterion (5), there does not exist a relation corresponding to such variance decomposition theorem. Nevertheless, this should not be the reason sufficient for the preference of the criterion (4) to the criterion (5). Besides that, for the completeness of our understanding on the problem of variance-based thresholding, we should appreciate the mechanism of the thresholding process and comprehend the factors as well as their ways to affect the process. To that end, the features of the MCVT and the Otsu methods are analyzed as follows.

2.1. Analysis of the MCVT method

To understand the decision process of the minimum class variance thresholding, we can investigate the impact of changing the membership of r_k on the cost $J_{\mathrm{MCVT}} = D_1 + D_2$. Suppose that r_k is changed to C_2. Denote the resulting classes as $C_1' = \{r_0, \ldots, r_{k-1}\}$ and $C_2' = \{r_k, \ldots, r_{L-1}\}$. The mean value of C_1' is

$$\mu_1' = \sum_{i=0}^{k-1} r_i h_i \Big/ P_1' = \mu_1 + h_k(\mu_1 - r_k)/P_1', \tag{6}$$

where $P_1' = \sum_{i=0}^{k-1} h_i$. Then, we can derive the variance of C_1'

$$D_1' = D_1 + h_k\left[D_1 - \frac{P_1}{P_1'}(r_k - \mu_1)^2\right]\Big/ P_1'. \tag{7}$$

The proof is given in Appendix. Eq. (7) describes the impact of removing r_k on the class variance of C_1, from which it is possible to design a fast algorithm for implementation in the similar fashion to Sund and Eilertsen (2003).

What is of interest here is the threshold-decision process of the MCVT method, from which we hope to understand the factors that play roles. For clarity, we define the change of class-variance as

$$\Delta D_1 = D_1 - D_1' = h_k\left[\frac{P_1}{P_1'}(r_k - \mu_1)^2 - D_1\right]\Big/ P_1' \tag{8}$$

From Eq. (8), we note that ΔD_1 depends on the difference between D_1 and $\frac{P_1}{P_1'}(r_k - \mu_1)^2$, in which the former characterizes the average distance of the C_1 data to its centroid and the latter stands for the weighted distance of r_k to the centroid of C_1. Therefore, ΔD_1 relies on the *relative distance* of r_k to the centroid of C_1. In Eq. (8), this relative distance is weighted by h_k and divided by P_1', the latter of which can be interpreted as the *average* relative distance of r_k to the centroid of C_1.

Similarly,

$$D_2' = D_2 + h_k\left[\frac{P_2}{P_2'}(r_k - \mu_2)^2 - D_2\right]\Big/ P_2'. \tag{9}$$

Thus, the cost of the partition C_1' and C_2' by the MCVT method

$$J'_{\mathrm{MCVT}} = D_1' + D_2'. \tag{10}$$

The decision rule to assign r_k into C_2 would be

$$J'_{\mathrm{MCVT}} < J_{\mathrm{MCVT}}. \tag{11}$$

Substituted with Eqs. (7) and (9), the decision rule becomes

$$\left[\frac{P_1}{P_1'}(r_k - \mu_1)^2 - D_1\right]\Big/ P_1' > \left[\frac{P_2}{P_2'}(r_k - \mu_2)^2 - D_2\right]\Big/ P_2'. \tag{12}$$

From (12), we observe that the MCVT method assigns r_k into the class to whose centroid r_k has a smaller average relative distance.

2.2. Analysis of the Otsu method

To analyze the Otsu method, we can also compute its cost J'_{Otsu} of the partition C_1' and C_2'. For convenience, we denote $S_i = P_i D_i$ as the within-class variances of C_i and $S_i' = P_i' D_i'$ as the within-class variances of $C_i', i = 1, 2$. From Eqs. (7) and (9), we can directly derive

$$S_1' = S_1 - h_k \frac{P_1}{P_1'}(r_k - \mu_1)^2 \tag{13}$$

and

$$S_2' = S_2 + h_k \frac{P_2}{P_2'}(r_k - \mu_2)^2. \tag{14}$$

The decision rule to classify r_k to C_2 by the Otsu method is

$$S_1' + S_2' < S_1 + S_2. \tag{15}$$

Substituting Eqs. (13) and (14) for (15) yields

$$\frac{P_1}{P_1'}(r_k - \mu_1)^2 > \frac{P_2}{P_2'}(r_k - \mu_2)^2. \tag{16}$$

From (16), we see that for threshold selection the Otsu method mainly utilizes the distance of r_k to the centroid, which is weighted by P_i/P_i'. When $P_i/h_k \gg 1$, the ratio $P_i/P_i' \approx 1$. Therefore the Otsu method will classify r_k into the class to whose centroid the r_k has a smaller distance. For convenience, we call this weighted distance as the *absolute distance* of r_k to the centroid.

2.3. Comparison of the two methods

From the above analysis, the MCVT method exploits the average relative distance to decide the threshold, where the absolute distance of r_k to the centroid is firstly translated by the class variance, resulting in the relative distance, then divided by the class probability, leading to the average relative distance. Hence, the decision process of the MCVT method accounts for more information for threshold selection.

Assume that two classes are well separated with unequal variances. For a component with larger variance, the gray level at the tail would have larger absolute distance. Thus, the valley will have smaller absolute distance to the component with smaller variance. Consequently, part of the gray levels at the tail of the component with larger variance would be misclassified by the absolute distance criterion and result in the threshold shift to the component with larger variance. But if we use the distance relative to the class variance, this problem would be partly overcome because the class variance will impede the threshold towards the component with larger variance. Take two components with class variances 10 and 20 for example. For a gray level r_k around the valley, suppose its absolute distances to be 15 and 22. Then, the Otsu method will classify r_k to C_1. However, r_k will belong to C_2 according to the relative distance criterion, which would be more acceptable.

In real applications, it is often reasonable to assume the noise field is homogeneous or varies in a narrow range, hence the difference between the results by comparing the absolute distance and the relative distance could be small in practice. However, it is usually possible that the proportion of the object to the whole scene can be significantly different. Thus, the class probability would make a difference on the final threshold selection between the Otsu method and the MCVT method. A simple case to illustrate the rationale of *average* relative distance is that if we come with a tie over the distance criterion, then the average distance

criterion would assign r_k to the component with larger probability, which is also quite reasonable.

Specifically, we assume r_k to be the valley and the distribution of C_i follows the Gaussian. Then r_k satisfies

$$\frac{P_1}{\sigma_1}\exp\left\{-\frac{(r_k-\mu_1)^2}{2\sigma_1^2}\right\}=\frac{P_2}{\sigma_2}\exp\left\{-\frac{(r_k-\mu_2)^2}{2\sigma_2^2}\right\}, \tag{17}$$

where $\sigma_i^2 = D_i$ and $\sigma_1/\sigma_2 \approx 1$. From (17), we can deduce that the valley is closer to the component with smaller class probability. As analyzed above, this partition (C_1 and C_2) does not attain the minimum cost by the Otsu method, which will classify r_k to the component with smaller class probability. As a result, the Otsu threshold will shift towards the component with larger class probability.

When the distance is divided by the class probability, the force to drive the Otsu threshold towards the larger component would be weakened. On the one hand, the distance will push the valley to the smaller component, on the other hand, the class probability tends to classify the valley into the larger component. Therefore, the net effect of the average distance would possibly result in the threshold closer to the valley than that by the distance criterion only.

To summarize the comparison, we observe that the decision process of the Otsu and the MCVT methods depends on two factors, the class variance and the class probability. The Otsu method tends to shift the threshold from the valley towards the component with larger class variance or larger class probability. The MCVT method takes the relative distance to overcome the class variance effect and the average distance to attenuate the class probability effect.

2.4. Multi-level thresholding

Extension of bi-level MCVT to multi-level thresholding is straightforward. Suppose there are $m-1$ thresholds $\vec{T}=(T_1,\ldots,T_{m-1})$, where $r_0 < T_1 < \cdots < T_{m-1} < r_{L-1}$. Let $T_0 = r_0$, $T_m = r_{L-1}+1$, then an m-partition of Ω is defined as

$$C_i=\{r_k | r_k \in \Omega, T_{i-1} \leqslant r_k < T_i\}, \quad i=1,\ldots,m.$$

For each component C_i, the corresponding parameters can be computed by

$$P_i=\sum_{r_k=T_{i-1}}^{T_i} h_{r_k} \tag{18}$$

$$\mu_i=\sum_{r_k=T_{i-1}}^{T_i} r_k h_{r_k} \Big/ P_i \tag{19}$$

$$D_i=\sum_{r_k=T_{i-1}}^{T_i} (r_k-\mu_i)^2 h_{r_k} \Big/ P_i. \tag{20}$$

Then, the MCVT minimizes the cost $J_{\mathrm{MCVT}}(\vec{T})=\sum_{i=1}^{m} D_i$ and the optimal thresholds $\vec{T}_{\mathrm{MCVT}}$ is given by

$$J_{\mathrm{MCVT}}(\vec{T}_{\mathrm{MCVT}})=\min_{\vec{T}} J_{\mathrm{MCVT}}(\vec{T}). \tag{21}$$

3. Numerical experiments

To validate the above analysis, the two variance-based methods have been evaluated against a number of images. Since the size of exhaustive search is $(L-m)^{m-1}$, the simulated annealing (SA) algorithm (Kirkpatrick et al., 1983) is exploited in implementation in order to reduce the computation load. The SA algorithm can be seen as an analogy to the statistical mechanics of annealing solids, and for completeness it is briefly described in the following.

Let $\vec{T}^0=(T_1^0,\ldots,T_{m-1}^0)$ be a initial *configuration* with cost J^0. A random perturbation is generated by changing a randomly selected T_i^0 to T_i^0+1 or T_i^0-1. Then the cost for the new configuration is computed and denoted by J^1. Let $\delta^1 J = J^1 - J^0$. If $\delta^1 J < 0$, the resulting configuration is accepted as configuration $\vec{T}^1$, otherwise it will be accepted with probability $\exp(-\beta\delta^1 J)$, where β is a parameter to control the annealing rate. If the perturbation is rejected, $\vec{T}^1=\vec{T}^0$. And the process is iterated till convergence.

For comparison with other thresholding techniques, the fuzzy c-partition (FCP) (Cheng and Chen, 1999) and the minimum error (MinErr) (Kittler and Illingworth, 1986) methods are implemented, where the former is programmed as bi-level thresholding through direct searching for the optimal threshold, and the latter is coded as both bi-level thresholding using the algorithm in (Kittler and Illingworth, 1986) and multi-level thresholding using the expectation-maximization algorithm (Dempster et al., 1977).

We firstly evaluate using synthetic images, then present the tests with real images, which come from Bowyer et al. (2001).

3.1. Synthetic images

It is usually desirable to test the thresholding algorithm using the synthetic images for which the ideal threshold(s) can be identified directly. Figs. 1 and 2 show two synthetic images with two and three components respectively, where going clockwise from upper left are the original image, the histogram, the MCVT result and the Otsu result. For the two-component synthetic image (Fig. 1), the valley is at 123. The threshold by the MCVT method is exactly the valley, whereas that by the Otsu method is 112. From the thresholded images, one can see that the Otsu method leads to a cleaner segmentation map in the smaller component, but more noisy in the larger component. For the three-component synthetic image, the valleys are at (69,177). The MCVT method determines the thresholds as (75,174), and the thresholds selected by the Otsu method are (85,162). From the histogram, it is clear that the MCVT method is more accurate in valley detection and the bias by the Otsu method resulted from the class variance or the class probability is obvious, which verifies the analysis in Section 2. In the thresholded images, the Otsu method almost perfectly segments the two smaller

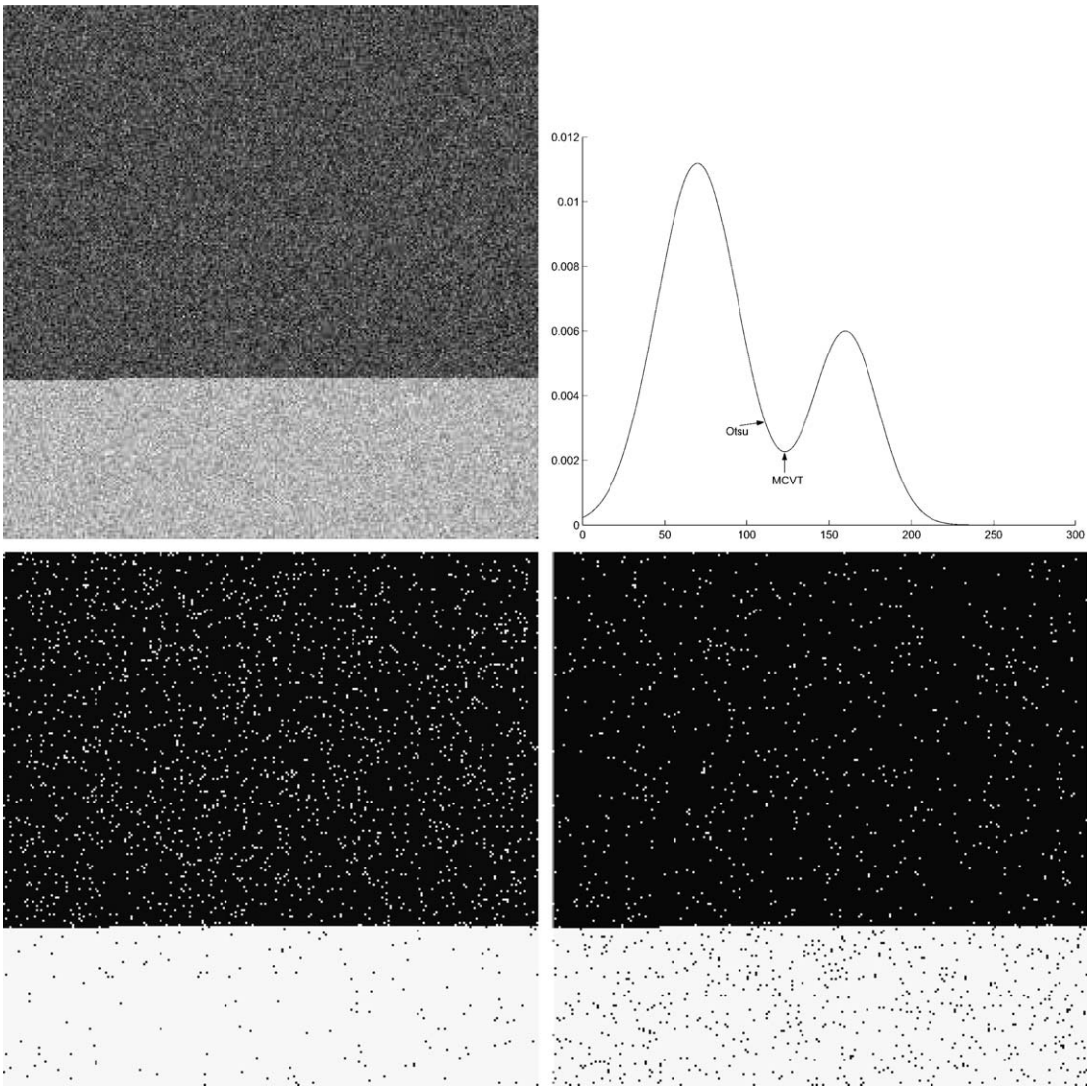

Fig. 1. Clockwise from upper left: a synthetic two component image, the histogram, the MCVT thresholded image and the Otsu thresholded image.

components, but yields a more noisy map in the largest component.

3.2. Real images

Fig. 3 presents the bi-level thresholding results of the Extinguisher image (1st row, left), where in the 2nd row are the MCVT result with threshold 78 (left) and the Otsu result with threshold 99 (right), and in the 3rd row are the FCP result with threshold 115 (left) and the MinErr result with threshold 164 (right). From the gray-level histogram (1st row, right), the picture roughly consists of the extinguisher and its background, the probability of the former is much smaller than that of the latter. The Otsu threshold shifts from the valley towards the larger component, which is consistent with the analysis in the above section. Comparatively, the MCVT threshold is closer to the valley. This observation can also be justified by comparing the thresholded results perceptually. The MCVT method is visually better in differentiating the extinguisher and the text from the background. It is also noted that the Otsu method misclassifies some background on the wall as the object. This effect is more pronounced in the FCP thresholded image, whose threshold shifts further toward the larger component. As for the MinErr result, the reported threshold is evidently far away from the ideal one. This may be due to the intensity outliers in the picture and a robustized version of the method may improve the result in this situation.

Fig. 4 displays the five-level thresholding results of the Iron image (1st row, left), where in the 2nd row left is the MCVT result with thresholds (101, 159, 189, 238) and right the Otsu result with thresholds (89, 154, 195, 230). Comparing the two thresholded results, we note that there are slightly larger portion of the wall being misclassified by the Otsu method (above the table on the right), and the objects (the table cloth over the table and that beside the table) detected by the MCVT method are more homogeneous. By examining the gray-level histogram (3rd row),

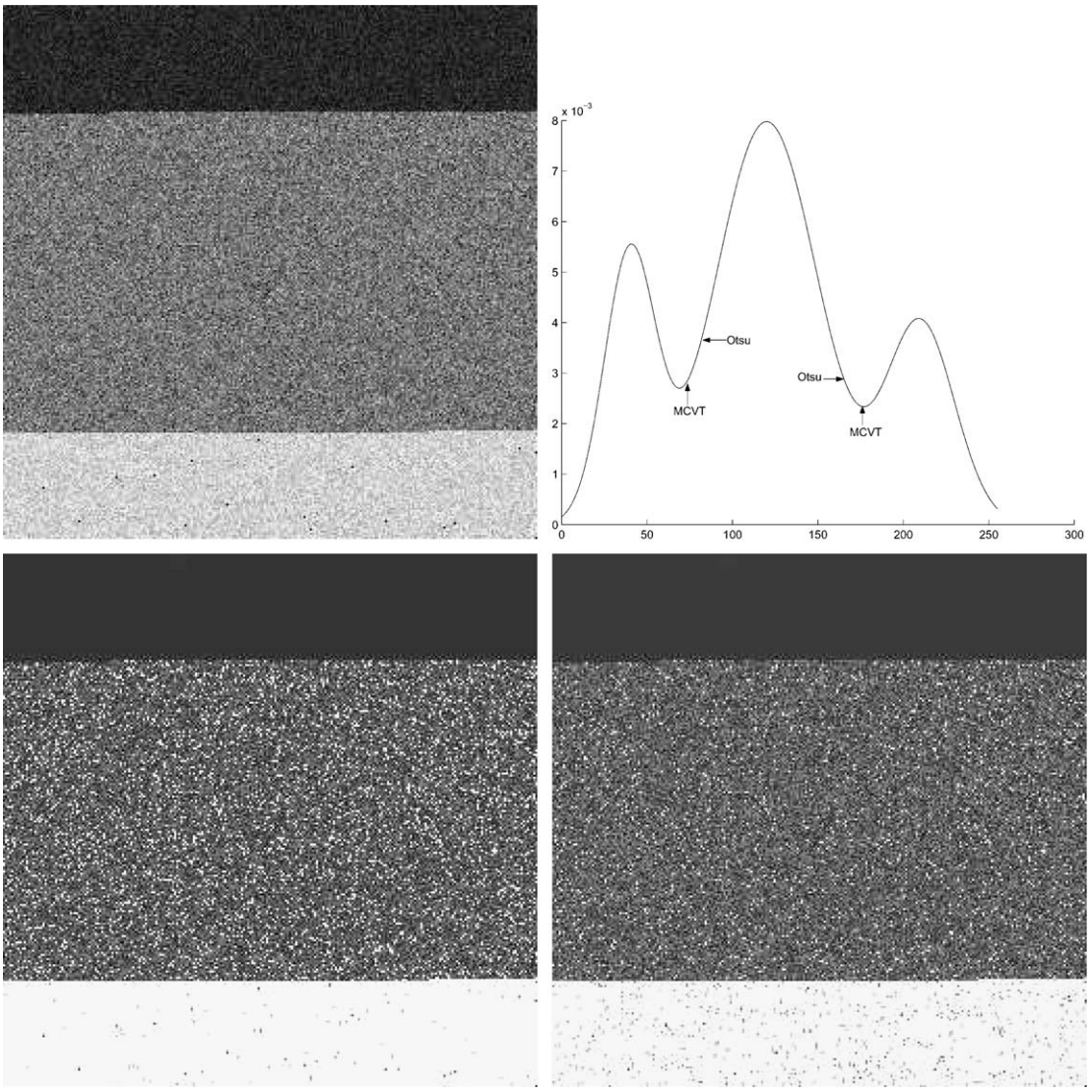

Fig. 2. Clockwise from upper left: a synthetic three component image, the histogram, the MCVT thresholded image and the Otsu thresholded image.

we can see that these effects are due to the class-probability effect of the Otsu method, which labels more tails of the largest component as other components. For comparison with other methods, the MinErr result is given in the 1st row (right), which is less satisfactory in object delineation.

Fig. 5 shows the application to an aerial image, the Woods image, with three-level thresholding. The MCVT result is in the 2nd row (left) with thresholds (72, 168), whereas the Otsu result on the right with thresholds (80, 150). From the histogram (3rd row), it can be seen that the picture consists of three components. The darkest component mainly corresponds to the trees and the shadow of buildings. The brightest component is largely contributed by the buildings and the roads. The middle component is dominated by the grassland. The three components are quite well separated and the MCVT solution is closer to the valleys. Comparatively, the Otsu solution misclassifies portions of grassland as Component 1 or Component 2. This can be clearer by examining the thresholded results directly. Evidently, the grassland identified by the Otsu method looks pretty noisy, comprising many randomly distributed holes which belong to Component 1 or Component 2. Again, these results are because of the class variance and the class probability effects of the Otsu method. The MinErr result is given in Row 1 (right) for a comparison, and the thresholds are (72, 155), the first of which is the same with that by the MCVT method but the second deviates further from the second valley toward the largest component. Thus the map of grassland is similar to that by the Otsu method.

Fig. 6 is another example on an aerial image of a school, with five-level thresholding. The MCVT result is on the left of Row 2 with thresholds (51, 93, 122, 178), and the Otsu result on the right with thresholds (58, 98, 130, 170). From the histogram (Row 3), the first valley is easy to identify, about 50–52. The Otsu threshold is 58, which is slightly larger. Hence, in the thresholded images, Component 2 (the second darkest) by the Otsu method contains more

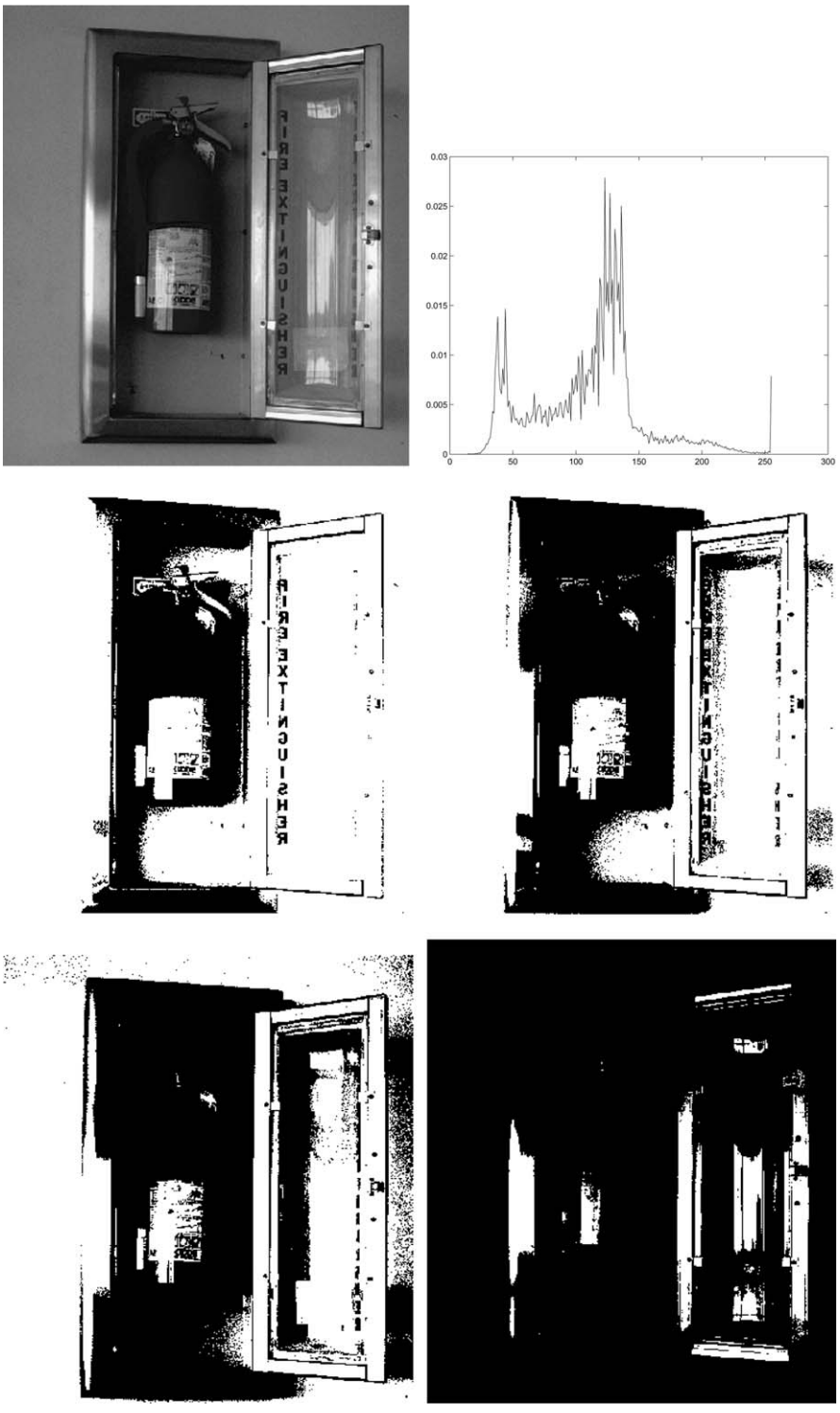

Fig. 3. Row 1: the original extinguisher image (left) and the histogram (right); Row 2: the MCVT bi-level thresholed result (left) with threshold 78 and the Otsu result (right) with threshold 99; Row 3: the FCP result (left) with threshold 115 and the MinErr result (right) with threshold 164.

Component 1 (the darkest, mainly composed of building shadow and trees) regions. Also from the histogram, the picture is dominated by Component 4, largely the buildings. The Otsu method cuts larger tails (from both the left and the right) of Component 4 as other components, which verifies the analysis as aforementioned. Consequently, Component 4 by the Otsu method is noisier and less homogeneous. For the building at the upper left corner, there is a much larger part which is identified by the Otsu method as Component 3. The MinErr result is shown in Row 1 (right) with thresholds $(51, 95, 131, 164)$. The first two thresholds locate very close to the valleys, but for the latter two, it

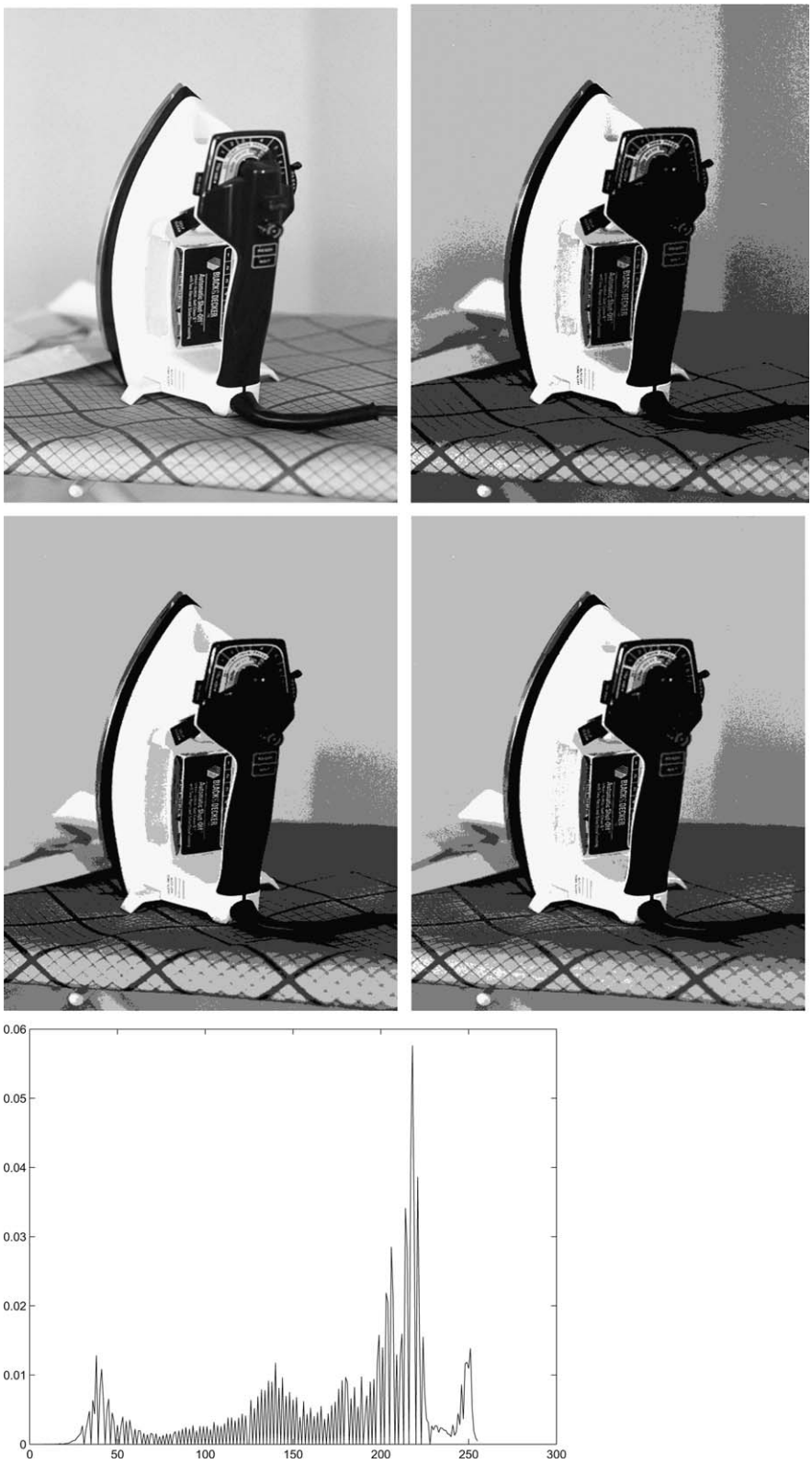

Fig. 4. Row 1: the original iron image (left) and the MinErr five-level thresholded result (right) with thresholds (102, 183, 211, 233); Row 2: the MCVT result (left) with thresholds (101, 159, 189, 238), and the Otsu result (right) with thresholds (89, 154, 195, 230); Row 3: the histogram.

is similar to the Otsu method in segmenting a portion of larger components as the neighbouring smaller ones in the histogram. In contrast, the MCVT method tends to preserve the shape of larger component.

An application to an MRI head image is presented in Fig. 7. The original image is on the top left and the region of interest (ROI) is on the top right. The ROI refers to the space enclosed by the skull and Hu et al. (2006) details on

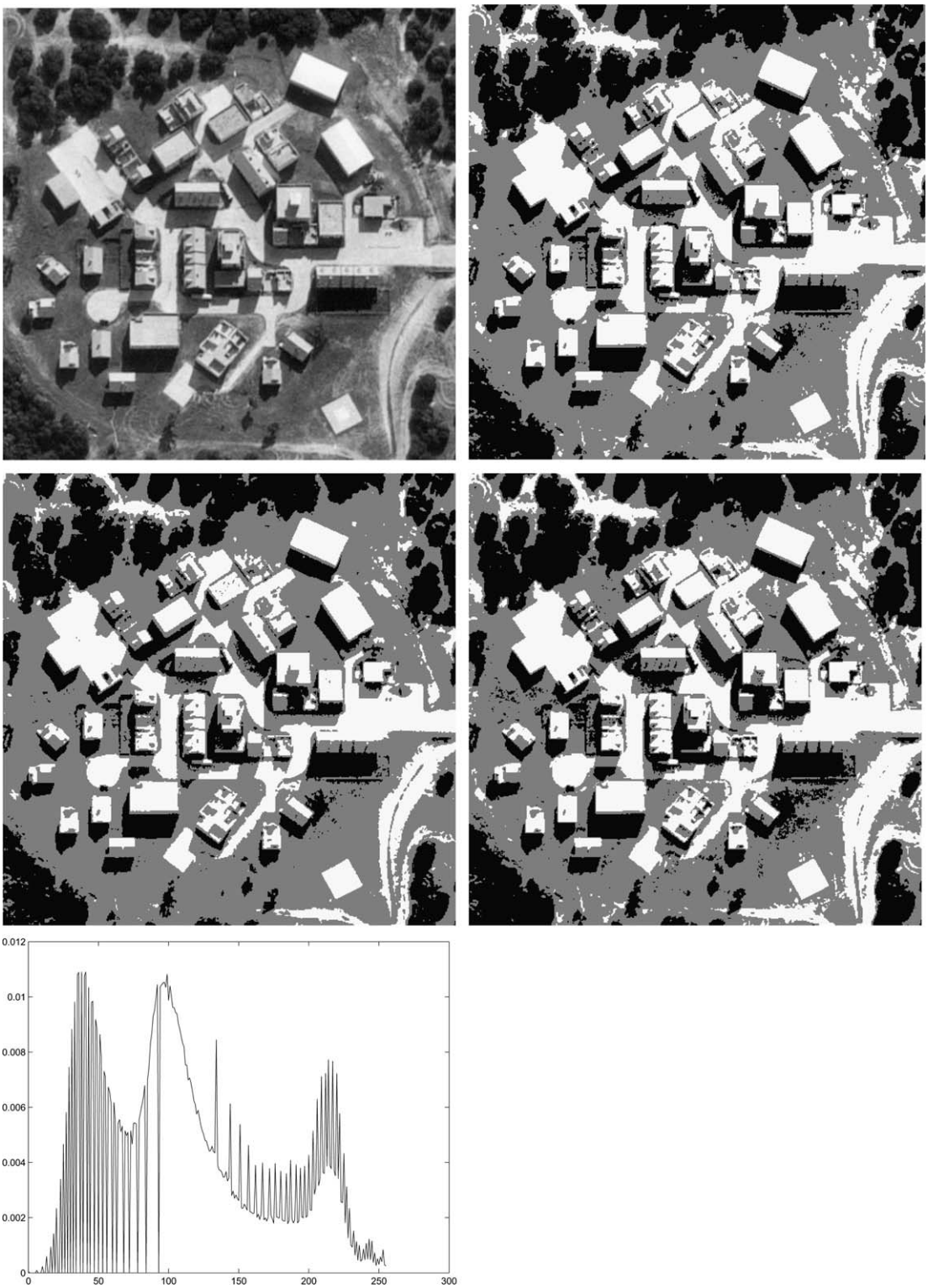

Fig. 5. Row 1: the original woods image (left) and the MinErr three-level thresholded result (right) with thresholds (72, 155); Row 2: the MCVT result (left) with thresholds (72, 168), and the Otsu result (right) with thresholds (80, 150); Row 3: the histogram.

deriving the ROI. The problem then is to remove the skull/scalp for brain tissue segmentation. To that end, we can use the thresholding method to separate the cerebrospinal fluid from the white matter and the gray matter. After that, the brain tissue can be isolated from the skull/scalp by morphological and connected-component analysis. The second row of Fig. 7 shows the thresholded results by the MCVT method (left) and the Otsu method (right). It is evident that the Otsu method is over-segmented, which classifies some gray matter as the cerebrospinal fluid. From

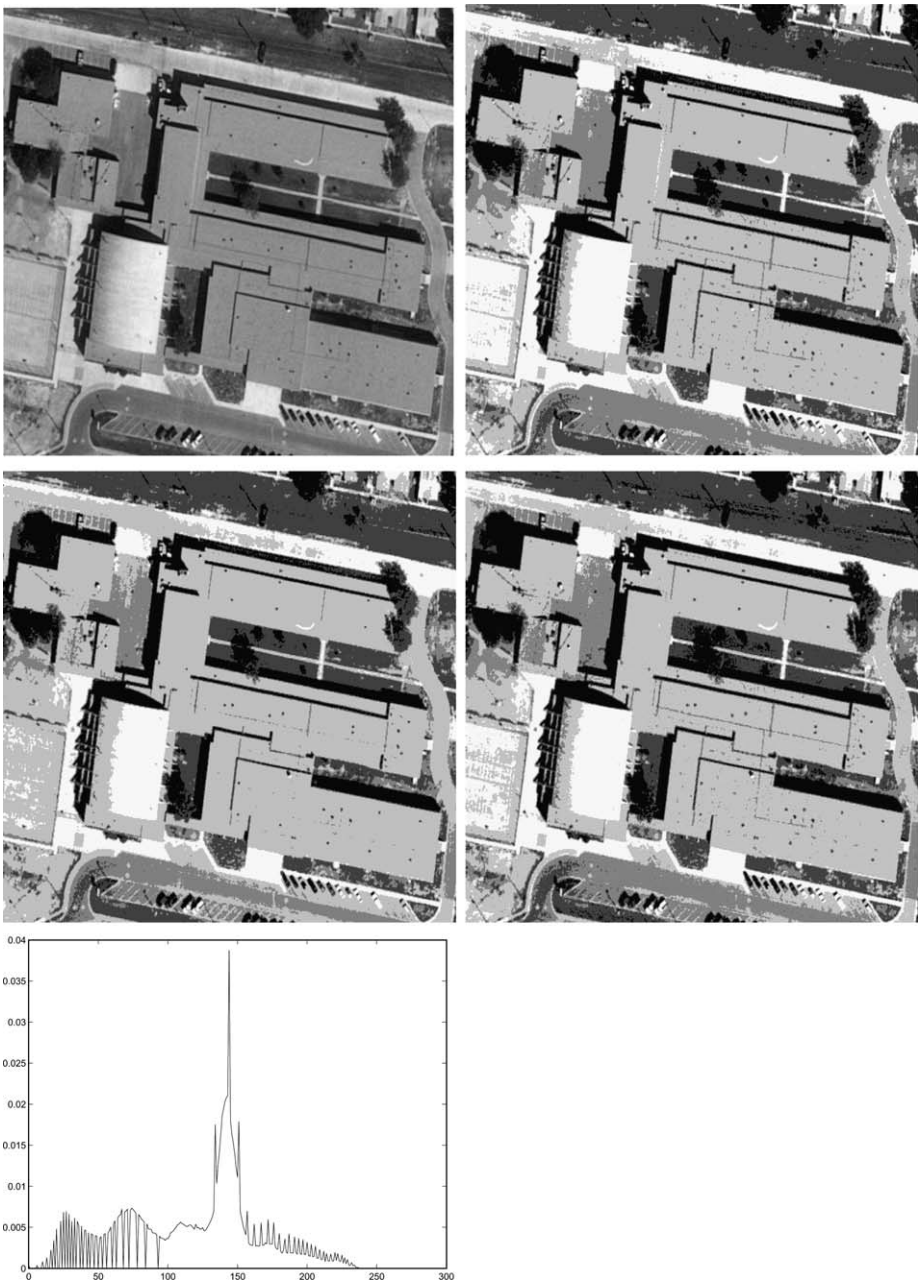

Fig. 6. Row 1: the original school image (left) and the MinErr five-level thresholded result (right) with thresholds (51, 95, 131, 164); Row 2: the MCVT result (left) with thresholds (51, 93, 122, 178), and the Otsu result (right) with thresholds (58, 98, 130, 170); Row 3: the histogram.

the gray-level histogram of the ROI (on the bottom left of Fig. 7), we can see that two peaks can be distinguished: the left smaller component corresponds to the cerebrospinal fluid and the right larger component is mainly contributed by the white matter, the gray matter and the skull/scalp. It is noticed that the left peak is much smaller than the right one. From our analysis, the Otsu method tends to shift the threshold towards the larger component, hence, it is not surprising to see that Otsu method misclassifies some gray matter as the cerebrospinal fluid. The Otsu threshold is 71 and the MCVT threshold is 46. Comparatively, the MCVT result is more reasonable in this example. The MinErr method fails to report a threshold due to model bias. And the FCP result is given on the bottom right, where the large component effect is even worse than that of the Otsu method. In addition, the variance-based thresholding method has been compared with respect to the MinErr method (Kittler and Illingworth, 1986) and the FCP method (Cheng and Chen, 1999) against a database of magnetic resonance head images, and the results were reported in Hu et al. (2006). Interestingly, it is noted that the FCP method also displays the large component effect as similar to the Otsu method.

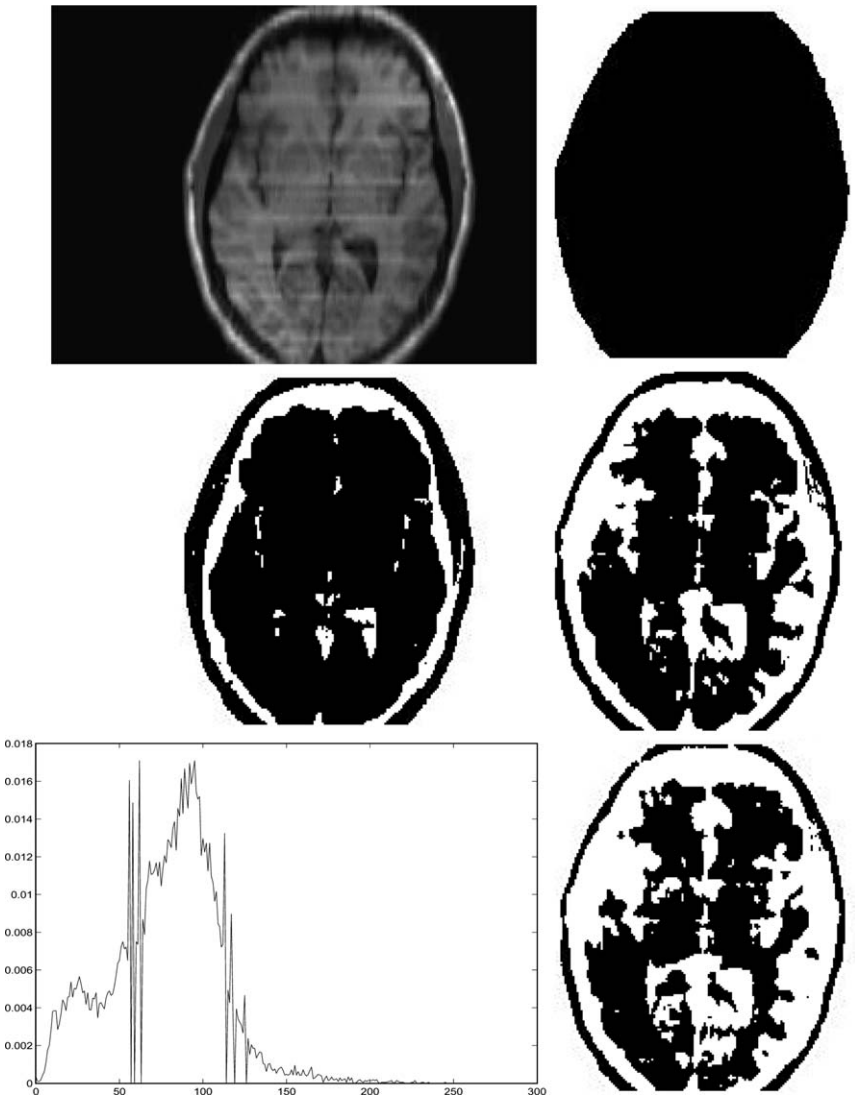

Fig. 7. On the top left is an original head MRI image and on the top right the ROI. The second row is the thresholded results by the MCVT method (left) and the Otsu method (right). The histogram is on the bottom left and the FCP result is on the bottom right.

4. Concluding remarks

In summary, we have presented in this paper an analysis on the mechanism of variance-based thresholding methods. Specifically, we have analyzed and compared the minimum class variance method and the minimum within-class variance method (the Otsu method). The analysis reveals that there are two factors, namely, class probability and class variance, which are critical for the performance of variance-based thresholding methods. These two factors play different roles in the MCVT and the Otsu methods. The Otsu method considers the absolute distances, whereas the MCVT method takes into account a more complete information including the absolute distances, the class variances and the class probabilities for threshold selection. In general, the Otsu method tends to shift the threshold towards the component with larger class probability or larger class variance. As for the MCVT method, there are two quantities to overcome the class probability and the class variance effects: the relative distance and the average distance. The former can attenuate the bias from the class variance and the latter can weaken the bias from the class probability. Experiments through synthetic and real images have verified the findings and illustrated that the MCVT method could be more accurate in valley detection than the Otsu method.

This paper has addressed the impact of class probability and class variance on the threshold selection of variance-based thresholding methods. There could exist factors like noise or inhomogeneity which could impose adverse effect on either the Otsu or the MCVT methods since these factors are not considered in the conventional design of thresholding methods. And this issue is beyond the scope of this paper. A special case which might be worth pointing out is the unimodal histogram thresholding, as often appeared in digital document images and fingerprint images. Generally, unimodal histogram images are not well defined for threshold-

ing because of the difficulty in differentiating the object from the background based only on the intensity information. There are special techniques for thresholding this type of images, for example Rosin (2001). From the analysis in Section 2, the Otsu method would give a quite "reasonable" threshold. It will separate the unique peak into two parts due to the variance decomposition theorem. However, no such corresponding decomposition for the class variance exists, so the MCVT method is not suitable for uni-modal histogram thresholding. Basically, the MCVT method behaves in the way very similar to the minimum Bayes error methods in preserving the modal shape of histogram.

Lastly, we would like to stress that this study not only analytically elaborates the bias generation in variance-based thresholding methods, but also provides a guidance on the selection of thresholding methods or the evaluation of the Otsu method for a specific image. In addition, this study also hints on how to improve the existing minimum variance thresholding methods using a better design of the anti-bias forces.

Appendix

By definition

$$\begin{aligned}
D_1' &= \frac{1}{P_1'}\sum_{i=0}^{k-1}(r_i-\mu_1')^2 h_i = \frac{1}{P_1'}\sum_{i=0}^{k-1}[(r_i-\mu_1)+(\mu_1-\mu_1')]^2 h_i \\
&= \frac{1}{P_1'}\sum_{i=0}^{k-1}[(r_i-\mu_1)^2+2(r_i-\mu_1)(\mu_1-\mu_1')+(\mu_1-\mu_1')^2]h_i \\
&= \frac{P_1}{P_1'}\left[\frac{1}{P_1}\sum_{i=0}^{k}(r_i-\mu_1)^2 h_i - \frac{h_k}{P_1}(r_k-\mu_1)^2\right] \\
&\quad + \frac{2}{P_1'}(\mu_1-\mu_1')\left[\sum_{i=0}^{k}(r_i-\mu_1)h_i-(r_k-\mu_1)h_k\right] \\
&\quad + \frac{(\mu_1-\mu_1')^2}{P_1'}\sum_{i=0}^{k-1}h_i.
\end{aligned}$$

According to Eqs. (1)–(3) and (6),

$$\begin{aligned}
D_1' &= \frac{P_1}{P_1'}D_1 - \frac{h_k}{P_1'}(r_k-\mu_1)^2 - 2\left(\frac{h_k}{P_1'}\right)^2(r_k-\mu_1)^2 \\
&\quad + \left(\frac{h_k}{P_1'}\right)^2(r_k-\mu_1)^2 \\
&= D_1 + \frac{h_k}{P_1'}D_1 - \frac{h_k P_1' + h_k^2}{(P_1')^2}(r_k-\mu_1)^2 \\
&= D_1 + h_k\left[D_1 - \frac{P_1}{P_1'}(r_k-\mu_1)^2\right]\Big/P_1'.
\end{aligned}$$

References

Bowyer, K., Kranenburg, C., Dougherty, S., 2001. Edge detector evaluation using empirical ROC curves. Comput. Image and Vision Understanding 84, 77–103.

Chang, Y., Fu, Alan M.N., Yan, H., Zhao, M., 2002. Efficient two-level image thresholding method based on Bayesian formulation and the maximum entropy principle. Optical Eng. 41, 2487–2498.

Cheng, H.D., Chen, Y., 1999. Fuzzy partition of two-dimensional histogram and its application to thresholding. Patter Recognition 32, 825–843.

Cho, S., Haralick, R., Yi, S., 1989. Improvement of Kittler and Illingworth's minimum error thresholding. Pattern Recognition 22, 609–617.

Chow, C.K., Kaneko, T., 1972. Automatic boundary detection of the left ventricle from cineangiograms. Comput. Biomed. Res. 5, 388–410.

Dempster, A.P., Larid, N.M., Rubin, D.B., 1977. Maximum likelihood from incomplete data via the EM-algorithm. J. Roy. Statist. Soc. B 39, 1–38.

Hu, Q.M., Hou, Z., Nowinski, W.L., 2006. Supervised range-constrained thresholding. IEEE Trans. Image Process. 15, 228–240.

Huang, L.K., Wang, M.J., 1995. Image thresholding by minimizing the measure of fuzziness. Pattern Recognition 28, 41–51.

Kirkpatrick, S., Gelatt, C.D., Vecchi, M.P., 1983. Optimization by simulated annealing. Science 220, 671–680.

Kittler, J., Illingworth, J., 1986. Minimum error thresholding. Pattern Recognition 19, 41–47.

Kurz, L., Benteftifa, M.H., 1997. Analysis of Variance in Statistical Image Processing. Cambridge University Press, Cambridge.

Li, C.H., Lee, C.K., 1996. Minimum cross entropy thresholding. Pattern Recognition 26, 617–625.

Nakagawa, Y., Rosenfeld, A., 1979. Some experiments on variable thresholding. Pattern Recognition 11, 191–204.

Otsu, N., 1979. A threshold selection method from gray-level histograms. IEEE Trans. Systems Man Cybernet. 9, 62–66.

Prewitt, J.M.S., Mendelsohn, M.L., 1966. The analysis of cell images. Ann. N.Y. Acad. Sci. 128, 1035–1053.

Pun, T., 1981. Entropic thresholding: A new approach. CVGIP 16, 210–239.

Rosenfeld, A., Torre, P.D.L., 1983. Histogram concavity analysis as an aid in threshold selection. IEEE Trans. Systems Man Cybernet. 13, 231–235.

Rosin, P.L., 2001. Unimodal thresholding. Pattern Recognition 34, 2083–2096.

Saha, P.K., Udupa, J.K., 2001. Optimum image thresholding via class uncertainty and region homogeneity. IEEE Trans. Pattern Anal. Machine Intell. 23, 689–706.

Shanbhag, A.G., 1994. Utilization of information measure as a means of image thresholding. CVGIP: Graphical Models and Image Processing 56, 414–419.

Sund, T., Eilertsen, K., 2003. An algorithm for fast adaptive image binarization with applications in radiotherapy imaging. IEEE Trans. Medical Imaging 22, 22–28.

Tobias, O.J., Seara, R., 2002. Image segmentation by histogram thresholding using fuzzy sets. IEEE Trans. Image Process. 11, 1457–1465.

Tsai, W., 1985. Moment-preserving thresholding: A new approach. CVGIP 29, 377–393.

Wang, Q., Chi, Z., Zhao, R., 2002. Image thresholding by maximizing the index of non-fuzziness of the 2-D gray-scale histogram. Comput. Image and Vision Understanding 85, 100–116.

Weszka, J.S., Rosenfeld, A., 1979. Histogram modification for threshold selection. IEEE Trans. Systems Man, Cybernet. 9, 38–52.

Wong, A.K.C., Sahoo, P.K., 1989. A gray-level threshold selection method based on maximum entropy principle. IEEE Trans. Systems Man and Cybernet. 19, 866–871.

Wu, V., Manmatha, R., 1988. Document image clean-up and binarization. In: Proc. SPIE'98 Document Recognition, vol. V, pp. 263–273.

Yan, H., 1996. Unified formulation of a class of image thresholding techniques. Pattern Recognition 29, 2025–2032.

Ye, Q., Danielsson, P., 1988. On minimum error thresholding and its implementations. Pattern Recognition Lett. 7, 201–206.